ACS APPLIED MATERIALS & INTERFACES

Research Article

www.acsami.org

Suspended Aminosilanized Graphene Oxide Nanosheets for Selective Preconcentration of Lead Ions and Ultrasensitive Determination by Electrothermal Atomic Absorption Spectrometry

Rafal Sitko,*[,†] Paulina Janik,[†] Barbara Feist,[†] Ewa Talik,[‡] and Anna Gagor[§]

[†]Institute of Chemistry and [‡]Institute of Physics, University of Silesia, Katowice, Poland

[§]Institute of Low Temperature and Structure Research, Polish Academy of Sciences, P.O. Box 1410, 50-950 Wroclaw, Poland

ABSTRACT: The aminosilanized graphene oxide (GO-NH_2) was prepared for selective adsorption of Pb(II) ions. Graphene oxide (GO) and GO-NH_2 prepared through the aminosilanization of GO with 3-aminopropyltriethoxysilane were characterized by scanning electron microscopy, powder X-ray diffraction, X-ray photoelectron spectroscopy, and Raman spectroscopy. The batch experiments show that GO-NH_2 is characterized by high selectivity toward Pb(II) ions. Adsorption isotherms suggest that sorption of Pb(II) on GO-NH_2 nanosheets is monolayer coverage, and adsorption is controlled by a chemical process involving the surface complexation of Pb(II) ions with the nitrogen-containing groups on the surface of GO-NH_2. Pb(II) ions can be quantitatively adsorbed at pH 6 with maximum adsorption capacity of 96 mg g^{-1}. The GO-NH_2 was used for selective and sensitive determination of Pb(II) ions by electrothermal atomic absorption spectrometry (ET-AAS). The preconcentration of Pb(II) ions is based on dispersive micro solid-phase extraction in which the suspended GO-NH_2 is rapidly injected into analyzed water sample. Such features of GO-NH_2 nanosheets as wrinkled structure, softness, flexibility, and excellent dispersibility in water allow achieving very good contact with analyzed solution, and adsorption of Pb(II) ions is very fast. The experiment shows that after separation of the solid phase, the suspension of GO-NH_2 with adsorbed Pb(II) ions can be directly injected into the graphite tube and analyzed by ET-AAS. The GO-NH_2 is characterized by high selectivity toward Pb(II) ions and can be successfully used for analysis of various water samples with excellent enrichment factors of 100 and detection limits of 9.4 ng L^{-1}.

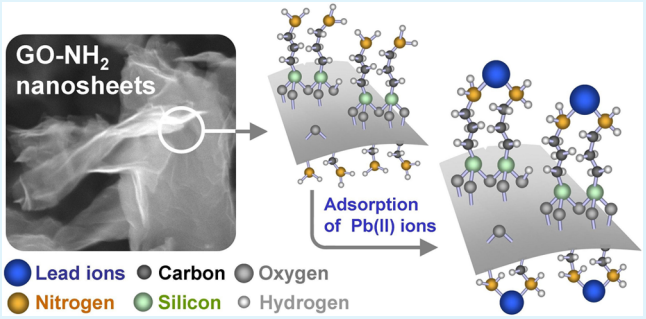

KEYWORDS: *preconcentration, solid-phase extraction, graphene, solid adsorbent, nanomaterial, environmental analysis*

1. INTRODUCTION

Since the first experimental evidence of the electronic properties of graphene in 2004,[1] graphene seems to be the most intensively studied material. Such a huge growth of interest in graphene can be explained by its exceptional electrical, electrochemical, optical, and mechanical properties. Graphene consists of sp^2-hybrydized carbon atoms organized in regular hexagonal layers, which make it chemically stable, flexible, corrosion resistant and durable.[2] Because of its unique structure and properties graphene is explored in a wide range of applications in electronics and optoelectronics,[3,4] chemical and biological sensors,[5] electrochemistry,[6] catalysis,[7] and in energy-related areas.[8] The past few years also show a huge growth of interest in graphene as a new adsorbent for removal of organic compounds.[9−12] Excellent adsorptive properties of graphene result from its huge surface area and its hexagonal arrays of carbon atoms that are ideal for strong interactions with other molecules due to the very large delocalized π-electron system. Such properties make graphene a very attractive adsorbent not only for pollution cleanup but also in solid-phase extraction (SPE) and solid-phase microextraction (SPME) in analytical chemistry.[13−16] However, graphene has extremely hydrophobic properties, and in consequence the metal ions present in hydrated forms or as complexes associated with simple anions cannot be adsorbed on graphene nanosheets. For this purpose, graphene oxide (GO) can be applied due to its extremely hydrophilic properties and the presence of functional groups containing oxygen atoms. These functional groups present on the surface of GO nanosheets can efficiently bind the metal ions to form a metal complex thanks to the fact of sharing an electron pair. The literature shows that GO has impressive adsorption capacities toward Co(II),[17] Cu(II),[18,19] Zn(II),[19] Cd(II),[17,19] Eu(III),[20,21] U(VI),[21−23] and Pb(II).[19,24,25] For example, the maximum adsorption capacity of GO toward Pb(II) ions ranged from 328 to 1119 mg g^{-1} depending on adsorption conditions and synthesis of GO. Thus, the adsorption capacity of GO is much higher than that of any of the currently reported conventional adsorbents as well as

Received: August 25, 2014
Accepted: October 20, 2014
Published: October 20, 2014

carbon nanotubes (CNTs). This results from the huge surface area of GO and the high content of oxygen-containing functional groups. The oxygen content in GO can be up to 30 wt %, whereas oxidized CNTs contain oxygen at concentration usually lower than 5 wt %. Moreover, in contrast to CNTs, both surfaces of GO sheet are accessible for adsorption of metal ions.[13] In the case of CNTs, the inner walls are not responsible for the adsorption due to steric hindrance. GO can be modified through chemical functionalization or preparation of GO-based composites with metal oxides or chelating polymers to improve adsorption capacities and/or selectivity toward metal cations[25−32] or to make possible the adsorption of anionic forms of metals.[33−35] Another kind of GO modification is preparation of GO-based magnetic nanocomposites that can be easily separated from the aqueous solution using external magnetic field.[34−37]

Although GO has impressive adsorption capacities toward metal ions, it is not selective toward metal cation. Therefore, several metal cations can be adsorbed on GO surface from their mixture. In consequence, competitive adsorption is observed, and adsorption percentage depends on the difference in the affinity of metal ions toward GO.[19] In this paper, GO was modified through the amino-silanization with 3-aminopropyltriethoxysilane (APTES) for selective adsorption of Pb(II) ions. GO-NH_2 was characterized by microscopy and spectroscopy techniques. The adsorption of Pb(II) on GO-NH_2 nanosheets was investigated by batch experiment including influence of pH, kinetics, and Langmuir and Freundlich isotherm models. The adsorptive properties of GO-NH_2 indicate its potential application for selective and ultrasensitive determination of Pb(II) ions by electrothermal atomic absorption spectrometry (ET-AAS).

2. EXPERIMENTAL SECTION

2.1. Reagents and Solutions. Lead stock solution (1 mg mL^{-1} of Pb) and (3-aminopropyl)triethoxysilane (APTES, 99%) were purchased from Sigma-Aldrich; nitric acid (65%, Suprapur) was from Merck Millipore (Billerica, MA, USA); sulfuric acid (98%, p.a.), ethanol (p.a.), ammonium hydroxide solution (25%, p.a.), potassium manganate (p.a.), and sodium nitrate (p.a.) were from POCh (Gliwice, Poland). Standard solutions were diluted with high purity water obtained from Milli-Q system (Millipore, Molsheim, France). Certified reference material BCR-610 (groundwater) was obtained from The Institute for Reference Materials and Measurements of Joint Research Centre (Geel, Belgium), whereas LGC6016 (estuarine water) from LGC-Standards (Teddington, UK).

2.2. Synthesis of GO. GO was synthesized by Hummers' method:[38] Concentrated H_2SO_4 (70 mL) was added to a mixture of graphite flakes (3.0 g) and $NaNO_3$ (1.5 g). The mixture was cooled to 0 °C, and 9 g of $KMnO_4$ was added slowly in portions to keep the reaction temperature below 20 °C. Then, the mixture was warmed to 35 °C and stirred for 12 h. The reaction mixture was cooled to room temperature and poured onto ice (400 mL) with 30% H_2O_2 (3 mL). Then, the mixture was centrifuged at 5000 rpm. The solid product was washed 20 times with water and 30 times with 5% HCl. Each time, the solid was redispersed by ultrasonication and was collected by centrifugation. Next, the solid was rinsed with deionized water. The centrifugation and ultrasonication with a new portion of deionized water were recycled ca. 20 times until the solution was neutral. The obtained GO was dried at 100 °C.

2.3. Synthesis of GO-NH_2. GO-NH_2 was synthesized as follows:[39,40] the suspension of 1 g of GO in 300 mL of anhydrous ethanol was sonicated for 1 h. Then, 10 mL of APTES was added to the suspension. The mixture was heated to 70 °C in a water bath and refluxed for 4 h. The solid phase was collected by centrifugation and washed eight times with ethanol and eight times with water to remove the residual APTES. Each time, the solid was redispersed by ultrasonication and was collected by centrifugation. The obtained GO-NH_2 was dried at 100 °C. GO-NH_2 suspension (5 mg mL^{-1} GO-NH_2) was prepared as follows: 125 mg of GO-NH_2 was sonicated for 60 min in 25 mL of high-purity water. To obtain homogeneous suspension, it was additionally sonicated for 5 min before every application.

2.4. Characterization of GO and GO-NH_2. Powder diffraction data (XRD) were collected on X'Pert PRO X-ray diffractometer with PIXcel ultrafast line detector and Soller slits for Cu Kα radiation. The measurements were done in Bragg−Brentano geometry. The Raman spectra were taken at room temperature using RenishawInVia Raman spectrometer equipped with confocal DM 2500 Leica optical microscope, a thermoelectrically cooled Ren Cam CCD as a detector, and a diode laser operating at 830 nm. The microstructural observations of the GO-NH_2 were conducted on a JEOL-7600F scanning electron microscope (SEM) equipped with the Oxford X-ray energy-dispersive spectrometer (EDS). The chemical composition of GO-NH_2 was confirmed by X-ray photoelectron spectroscopy (XPS). Photoelectron spectra were collected using a PHI 5700/660 Physical Electronic spectrometer with monochromated Al Kα radiation. The spectra were analyzed with a hemispherical mirror assuring energy resolution of ∼0.3 eV. Three hours after placing the samples in situ at 10^{-10} hPa vacuum, their surface was clean enough for measurements. The binding energy in the range −2 to 1400 eV and the core-level characteristic peaks for C 1s, O 1s, and N 1s were measured. The background was subtracted using the Tougaard approximation.

2.5. Batch Adsorption Experiment. The batch adsorption experiments were carried out with 1 mg of GO-NH_2 and 25 mL of Pb(II) aqueous solutions with the desired concentration and pH. The pH values of the suspensions were adjusted with nitric acid or ammonia solutions. Then, the suspensions were stirred within 5−120 min (kinetic study) or stirred for 90 min to achieve adsorption equilibrium (in the case of adsorption isotherms). The suspensions were filtered through a 0.45 μm membrane filter. The amount of Pb(II) ions adsorbed on GO-NH_2 (mg g^{-1}) calculated from the difference between the initial concentration C_0 (mg L^{-1}), and equilibrium concentration C_e (mg L^{-1}) was determined by the inductively coupled plasma atomic emission spectroscopy (ICP-OES) after filtration: $q_e=(C_0-C_e)V/m_{adsorbent}$, where V is the volume of the suspension, and $m_{adsorbent}$ is the mass of GO-NH_2.

2.6. Preconcentration Procedure. The pH of sample (50 mL) was adjusted to 6 using 0.1 mol L^{-1} HNO_3 and/or 0.1 mol L^{-1} NH_3. Then, 200 μL of GO-NH_2 suspension (5 mg mL^{-1} GO-NH_2) was injected into the analyzed solution and sonicated for 10 min. In the next step, the sample was passed through Millipore cellulose acetate membrane (0.45 μm) with the use of filtration assembly of 5 mm in diameter. Subsequently, the membrane filter with collected GO-NH_2 was placed in a 3 mL Eppendorf tube containing 0.5 mL of 2 mol L^{-1} HNO_3. The closed Eppendorf was placed in ultrasonic bath for 2 min. The redispersed GO-NH_2 can be injected directly into the graphite tube and analyzed by ET-AAS. The 2 mol L^{-1} HNO_3 containing eluted Pb(II) ions can also be separated via filtration or centrifugation from the GO-NH_2 solid phase and measured by ET-AAS.

The real water samples were collected in the Upper Silesia region of Poland. Before the preconcentration procedure described above, the water samples were filtered through a Millipore cellulose acetate membrane (0.45 μm) and then stabilized by acidification with concentrated nitric acid to achieve a pH of 2 (ca. 0.6−0.8 mL of HNO_3 per 1000 mL of water sample). The water samples were stored at 4 °C in polyethylene bottles.

2.7. Determination of Pb(II) by ET-AAS. ET-AAS measurements were performed with a Solaar M6 (TJA Solutions, Cambridge, U.K.) equipped with a Zeeman background corrector, an electrothermal atomizer, and an autosampler. The wavelengths were 217.0 nm with spectral band of 0.5 nm. The furnace temperature program is presented in Table 1. Aliquots or suspensions of 20 μL were injected directly into the graphite tube pyrolytically coated (Schunk Kohlenstofftechnik, Germany). The analysis was performed using 5 μL of $Mg(NO_3)_2$ as chemical modifier.

Table 1. Furnace Temperature Program

	temperature, °C	ramp, °C s^{-1}	hold, s	argon gas flow (L min^{-1})
drying	100	10	30	0.2
pyrolisis	800	150	20	0.2
atomization	1200		3	
cleaning	2500		3	0.2

3. RESULTS AND DISCUSSION

3.1. Characterization of GO and GO-NH_2. GO and GO-NH_2 were characterized by XRD, Raman spectroscopy, and XPS. Figure 1a presents XRD patterns of graphite, GO, and GO-NH_2. The most pronounced is the diffraction peak of graphite at $2\Theta = 26.5°$ that corresponds to coherently scattering hexagonal carbon layers with d_{002} spacing of 3.36 Å. In GO, the peak vanishes. Instead, broad and much less-intense peak appears at 13.14°. It matches the interlayer distance of 6.73 Å that results from intercalation of functional groups into the carbon sheets. The distance between the graphene oxide sheets in GO ranges from 5 to 9 Å and depends on the number and type of intercalated groups.[41] The number of the coherently scattering layers in GO that may be obtained from the D_{002}/d_{002} ratio is equal to ca. 7 (D_{002} is a thickness of GO in the stacking direction calculated from the Sherrer's formula, and d_{002} is the distance between hexagonal layers[42]). The thickness of GO in [002] direction is equal to ca. 5 nm, which is in contrast to ~60 nm graphite sheets. As far as the GO-NH_2 is concerned, the XRD patterns differ considerably from that of graphite and GO. The characteristic peaks vanish, and the broad hump extending from 10 to 30° with maximum at around 20 deg appears, indicating destruction of the long-range order in the stacking direction, which is equivalent to the exfoliation of the GO multilayers. It should be noted, however, that at 6.57° in GO-NH_2 new diffraction peak arises that is absent in graphite and GO. It matches the interlayer distance of 13.43 Å and probably results from the long-range order between functionalized GO.

The main features of the Raman spectra (Figure 1b) of graphite and GO are the so-called G and D peaks,[43] which lie at ~1582 and 1312 cm^{-1}, respectively, for excitation with 830 nm. The Raman spectrum of graphite consists of three bands. The most pronounced is the G band at 1582 cm^{-1} related to E_{2g} vibrational mode of ordered in-plane sp^2 carbons. Two disorder modes observed at 1312 cm^{-1} (D band) and 1613 cm^{-1} (small D′ shoulder band) are related to the disorder of edge carbons. Along the graphite to GO and GO-NH_2 path, the Raman spectrum undergoes changes that are similar to those observed in the graphite to nanocrystallite graphite transition.[44] The G band broadens significantly and displays a shift to higher frequencies from 1582 to 1600 cm^{-1}; the D band grows in intensity and broadens. Since the D peak is due to the breathing modes of the six-atom rings, it requires a defect for its activation.[45] It vanishes in the single crystals of graphite; thus, it is an indicator of disorder. Disorder manifests in broadening of G band as well as broadening and increase of the relative intensity of the D band compared to that of the G band. The intensity ratio I_D/I_G is generally accepted as a measure of the disorder in carbon structures.[45,46] In the studied materials, the measured I_D/I_G values of graphite, GO, and GO-NH_2 are 0.59, 1.4, and 1.34, respectively. Large I_D/I_G values in GO and GO-NH_2 confirm the presence of functional groups and additional disorder at the carbon edges. The blue G band shift in GO and GO-NH_2 originates from the alternating patterns of single–double carbon bonds within the sp^2 carbon ribbons.[47] The presence of the D′ band in the Raman spectrum of graphite is a signpost of a number of the edge carbons in the sample that may be related to the small size of the graphite sheets.

The synthesized GO-NH_2 was characterized by SEM and XPS. SEM image of synthesized GO-NH_2 is shown in Figure 2.

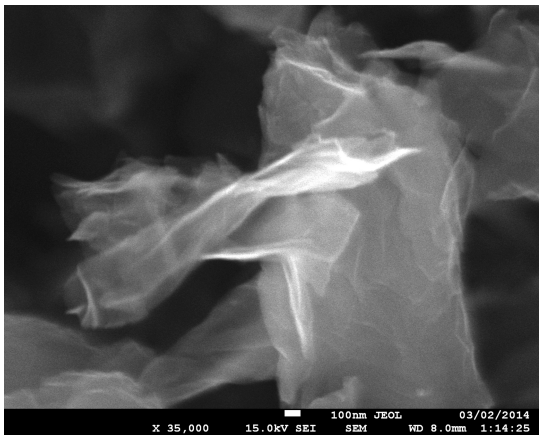

Figure 2. SEM image (35 000×) of synthesized GO-NH_2.

As can be seen, the highly wrinkled GO-NH_2 nanosheets are semitransparent, which suggests their few-layer nature. Such a wrinkled structure of GO-NH_2 can result in a large surface area and high extractive capacity. The synthesized GO-NH_2 was also

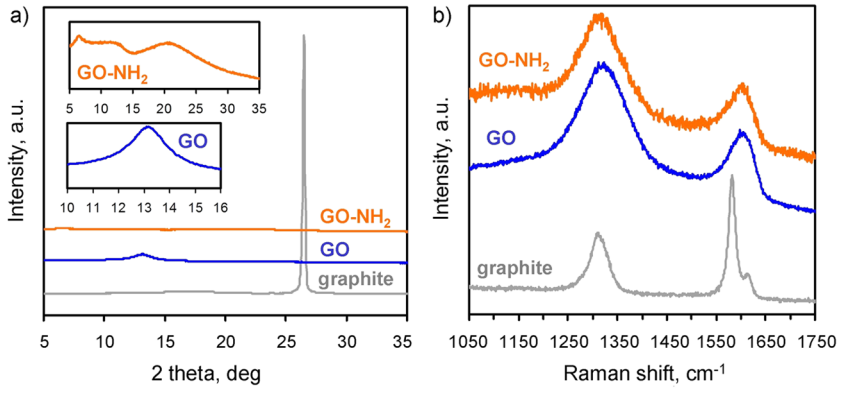

Figure 1. XRD patterns (a) and Raman spectra (b) obtained for graphite, GO, and GO-NH_2 samples.

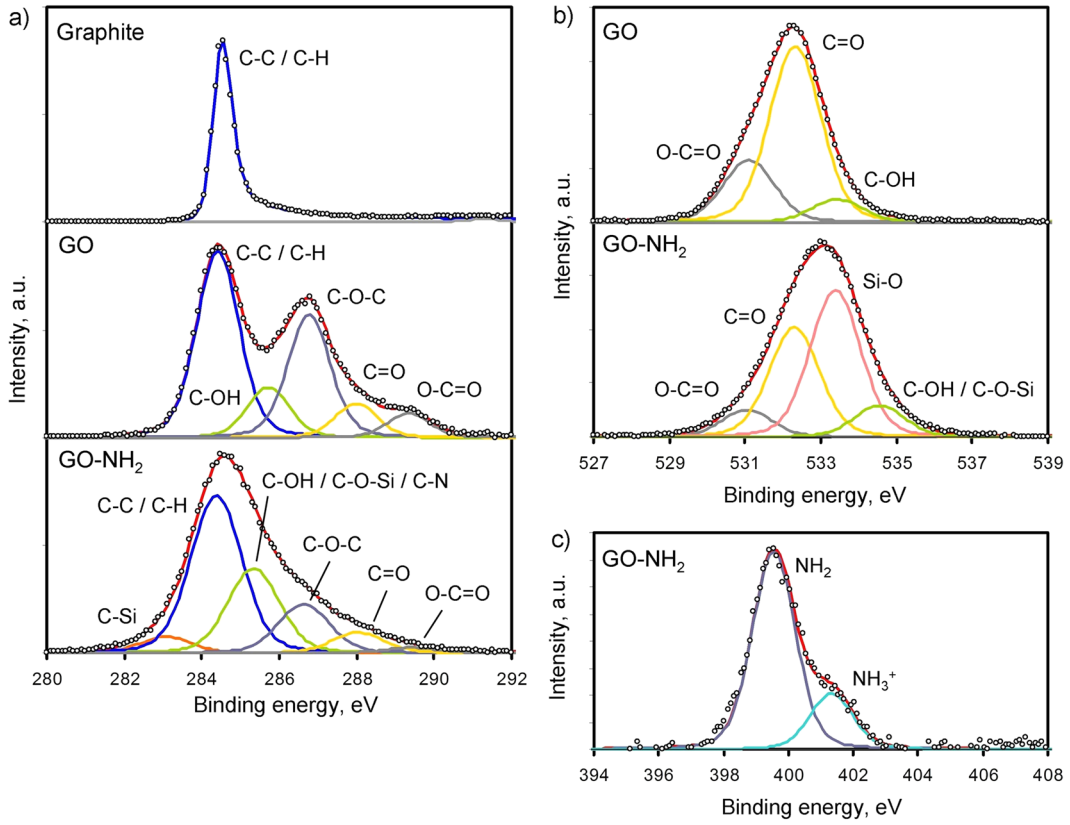

Figure 3. High-resolution XPS spectra of C 1s (a), O 1s (b), and N 1s (c) collected for graphite, GO, and GO-NH_2.

characterized by XPS. The high-resolution C 1s, O 1s, and N 1s spectra are presented in Figure 3. The C 1s spectrum of graphite shows the main peak at 284.4 eV due to the graphitic carbon, whereas spectrum of GO also reveals other four peaks at 285.8, 286.9, 288.1, and 289.5 eV assigned to C−OH, C−O−C, C═O, and O−C═O. The C 1s spectrum of GO-NH_2 was deconvoluted into six peaks at 283.1 eV (C−Si), 284.4 eV (C−C and C−H), 285.4 eV (C−OH, C−O−Si, C−N), 286.7 eV (C−O−C), 288.1 eV (C═O), and 289.5 eV (O−C═O).[48−51] The O 1s spectrum of GO shows the three peaks at 531.2, 532.4, and 533.6 eV assigned to O−C═O, C═O, and C−OH, whereas the O 1s spectrum of GO-NH_2 reveals four peaks at 531.2, 532.4, 533.5, and 534.7 eV assigned to O−C═O, C═O, Si−O, and C−OH/C−O−Si.[49,52] The N 1s spectrum of GO-NH_2 was deconvoluted into two peaks at 399.7 and 401.4 eV assigned to the free amino group ($-NH_2$) and the protonated amine ($-NH_3^+$).[50] Both C 1s and O 1s spectra indicate the successful modification of GO nanosheets with APTES. GO-NH_2 demonstrates new peaks at 283.1 eV (C−Si) and 533.5 eV (Si−O) other than those assigned to the GO surface functional groups. Also note here that the peak intensities and binding energies for GO and GO-NH_2 are slightly different. This results from the exposure of highly reactive hydroxyl and epoxy groups to the APTES. In consequence, the decrease in the epoxy and hydroxyl groups present on the surface, and simultaneously, new C−O−Si and C−N bonds contributing to the peak at 285.4 eV are observed.[49] The APTES is a bifunctional silane. Therefore, APTES can also be grafted to GO surface through a linkage between amine group in APTES and the carboxylic group on GO. However, the very small peak at 289.5 eV indicates that fraction of APTES that grafted to GO through the amine linkage is rather small. Therefore, APTES is attached to GO through hydroxyl and epoxy groups on GO surface.[48]

3.2. Adsorption of Pb(II) Ions on GO-NH_2. The acidity of the analyzed sample plays an important role in adsorption of metal ions, which results from two factors. First, it is related to the protonation and deprotonation of binding sites of the chelating molecules onto the surface of graphene nanosheets. Second, the adsorption depends on the metal species present in solution. The adsorption of Pb(II) ions on GO-NH_2 was investigated at pH ranging from 1 to 10. As shown in Figure 4,

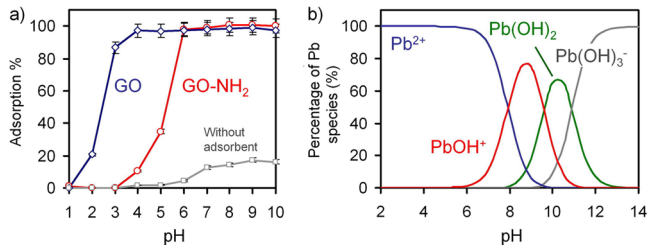

Figure 4. Effect of pH on the adsorption of Pb(II) ions on GO-NH_2 (a) and Pb(II) species at different pH (b); conditions: C_0 = 0.25 mg L^{-1}, $C_{GO\text{-}NH2}$ = 0.04 g L^{-1}, T = 25 °C, time = 90 min, the error bars correspond to one standard deviation, n = 3.

the adsorption of Pb(II) increases quickly at pH 5−6 and remains constant at pH 6−10. At pH 1−7, the predominant lead species are Pb^{2+}. However, the protons in acid solution can protonate binding sites of the chelating molecules onto the surface of GO-NH_2 (the point of zero charge pH_{PZC} of carbon surface modified with APTES is ca. 4.5[53] In consequence, the positive charges generated on the graphene surface (at pH <

dx.doi.org/10.1021/am505740d | ACS Appl. Mater. Interfaces 2014, 6, 20144−20153

pH_{PZC}) result in electrostatic repulsion. Moreover, the chelating mechanism is not possible. In neutral and basic solution, the favorite mechanism is the reaction between a lone pair of electrons in nitrogen of APTES and Pb^{2+} ion, which results in formation of metal complex. However, the Pb(II) ions begin to form a precipitate at pH 8−11 depending on initial metal concentration. Therefore, pH 6 was chosen as the optimum pH for further studies. To verify if the Pb(II) ions do not form a precipitate at pH 6, the experiment without GO-NH_2 was performed. As can be seen in Figure 4a, the contribution of precipitation of $Pb(OH)_2$ to adsorption of Pb(II) on GO-NH_2 is very low. Moreover, precipitation above pH 6 is insignificant due to low concentration of Pb(II) used in this experiment (C_0 = 0.25 mg L^{-1}). Therefore, the solubility product of $Pb(OH)_2$ (pK_{SP} = 14.84) is not exceeded, and precipitation does not occur. Figure 4a also shows the effect of pH on adsorption of Pb(II) ions on GO used as a precursor for synthesis of GO-NH_2. As can be observed, the adsorption of Pb(II) increases quickly at pH 2−4 and remains constant at pH 4−10. Thus, the adsorption of Pb(II) ions is shifted to lower value of pH. This can be explained by lower pH_{pzc} value (pH_{pzc} = 3.8−3.9 for GO nanosheets)[17,20,22,24] as well as by the by the strong surface complexation of Pb(II) ions with the oxygen-containing groups on the surface of GO.[19]

The contact time between the metal ions and the adsorbent is crucial to obtain high adsorption percentage. The kinetics of an adsorption process was studied using the pseudo-second-order[54] rate adsorption kinetic model:

$$\frac{1}{q_t} = \frac{1}{k_2 q_e^{\,2}} + \frac{t}{q_e}$$

where q_e and q_t (mg g^{-1}) are the capacities of Pb(II) adsorbed at equilibrium and time t (min), respectively, and k_2 is the pseudo-second-order rate constant (g mg^{-1} min^{-1}). The experimental data for adsorption of Pb(II) ions (C_0 = 1.0 mg L^{-1}) on GO-NH_2 nanosheets ($C_{GO\text{-}NH2}$ = 0.04 g L^{-1}) is very well-fitted by this kinetics model (r = 0.9982, q_e = 27.1 ± 1.9 mg g^{-1}, k_2 = 0.0046 ± 0.00055 g mg^{-1} min^{-1}). Moreover, the experimental q_e value (25 mg g^{-1}) is close to q_e value calculated from the pseudo-second-order kinetic models. Data of the pseudo-second-order kinetic model may indicate that the adsorption of Pb(II) on GO-NH_2 is controlled by chemisorption involving the surface complexation with the nitrogen-containing groups on the surface of GO. Therefore, the adsorption capacity is proportional to the number of active sites occupied on the GO-NH_2 nanosheets. It is worth noting here that the adsorption percentage is higher than 90% after 30 min, and adsorption at 99% level can be obtained after 60 min.

The adsorption of Pb(II) ions on GO-NH_2 was also simulated using Langmuir[55,56] and Freundlich[57] isotherm models:

$$q_e = \frac{q_{max} K_L C_e}{1 + K_L C_e}$$

$$q_e = K_F C_e^{1/n}$$

where q_{max} is the maximum amount of metal ions adsorbed per unit weight of GO-NH_2 at the high equilibrium ion concentration (mg g^{-1}), K_L is the constant related to the free energy of adsorption (L mg^{-1}), and K_F (mg^{1-n} L^n g^{-1}) and n are Freundlich constants related to the adsorption capacity and the adsorption intensity, respectively. The Langmuir and Freundlich adsorption isotherms for GO-NH_2 and GO used as precursor for GO-NH_2 synthesis are presented in Figure 5. Isotherm parameters were obtained by fitting the adsorption equilibrium data to the isotherm models.

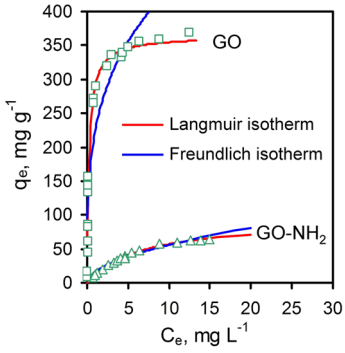

Figure 5. Langmuir and Freundlich adsorption isotherms; conditions: $C_{GO\text{-}NH2}$ = 0.04 g L^{-1}, C_{GO} = 0.04 g L^{-1}, pH = 6, T = 25 °C, time = 90 min.

It can be noticed that the adsorption isotherms are better fitted by the Langmuir model (r = 0.9973, K_L = 0.147 ± 0.008 L mg^{-1}, q_{max} = 96 ± 2.5 mg g^{-1}) than by the Freundlich model (r = 0.9841, K_F = 16 ± 1.0 mg^{1-n} L^n g^{-1}, n = 1.9 ± 0.10), which suggests a chemical adsorption process; that is, the Pb(II) ions can be chelated by the neighboring amino groups remaining onto the GO-NH_2 surface. The maximum adsorption capacity q_{max} of 96 ± 2.5 mg g^{-1} is lower than that for pure GO used as a precursor for synthesis of GO-NH_2 (q_{max} obtained by fitting the adsorption equilibrium data to the Langmuir model equals 364 ± 4.0 mg g^{-1}). However, the advantage of GO-NH_2 over GO is its high selectivity toward Pb(II) ions. The effect of pH on the adsorption of other metal ions was investigated to demonstrate selectivity of GO-NH_2. As can be seen in Figure 6, the adsorption of Cr(III), Cr(VI), Co(II), Ni(II), Cu(II), Zn(II), As(III) and Cd(II) at pH 6 is usually below 15%. The highest adsorption was obtained for Cu(II) and Cr(VI). However, the recoveries are not quantitative and equal 32 and 25%, respectively. The adsorption percentage of Cr(VI) at

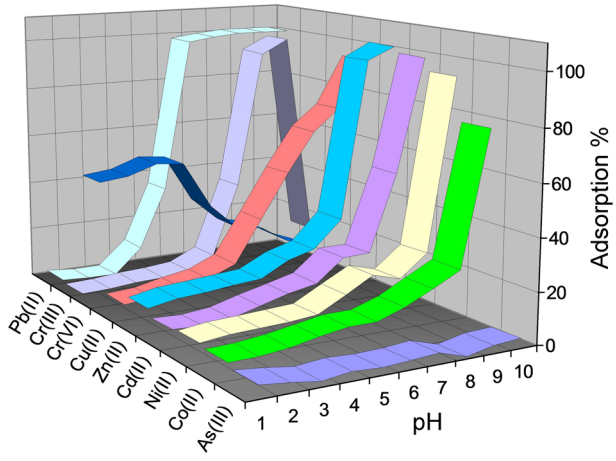

Figure 6. Effect of pH on adsorption of some metal ions on GO-NH_2; conditions: C_0 = 0.25 mg L^{-1}, $C_{GO\text{-}NH2}$ = 0.04 g L^{-1}, T = 25 °C, time = 90 min.

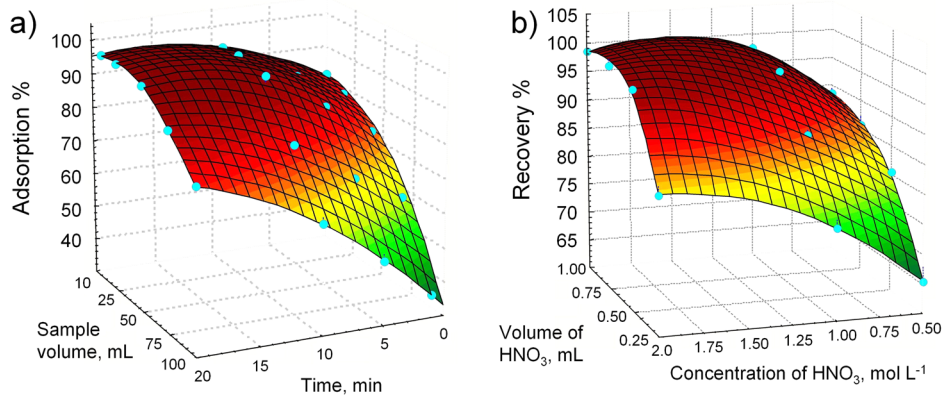

Figure 7. Effect of sample volume and time on adsorption of 12.5 ng of Pb(II) on 1 mg of GO-NH_2 (a) and effect of volume and concentration of HNO_3 on elution of Pb(II) ions (b).

pH 1−4 equals ca. 50−55%. Such significant value can be explained by the positive charges generated on GO-NH_2 surface due to the protonation of binding sites. In consequence, the electrostatic interactions between the anionic form of Cr(VI) and GO-NH_2 nanosheets become stronger. The high recoveries of Cr(III), Co(II), Ni(II), Cu(II), Zn(II), and Cd(II) can be observed at pH 8−10. This can be explained by the coprecipitation of metal hydroxides. However, a chelating mechanism is also possible. To summarize, the GO-NH_2 can be considered as highly selective toward Pb(II) ions at pH 6 and seems to be an ideal adsorbent for the trace analysis using single-element techniques, for example, ET-AAS. Moreover, q_{max} = 96 ± 2.5 mg g^{-1} can be considered as sufficient for the adsorption in SPE of trace Pb(II) ions.

3.3. Application of GO-NH_2 in DMSPE of Pb(II) Ions. In conventional solid-phase extraction (SPE), the liquid sample is passed through a column containing an adsorbent that retains the metal ions. However, the practical application of the GO-NH_2 nanosheets in SPE can be hampered. Very small particles of GO-NH_2 can escape from the SPE column. Moreover, they can cause high pressure in the SPE system. For these reasons, GO-NH_2 was applied in dispersive microsolid phase extraction (DMSPE) rather than in conventional SPE. In this case, the suspension of nanomaterial is injected into the analyzed aqueous sample. Thus, the small size of GO-NH_2 nanosheets, which cause serious problems in conventional SPE, can be considered as a great advantage in DMSPE.

The sample volume and contact time have a significant impact on the recovery of Pb(II) ions. The effect of the sample volume and contact time on the adsorption of Pb(II) ions was investigated by varying the sample volume from 10 to 100 mL and time from 0 to 20 min. As can be seen in Figure 7a, the adsorption percentage of Pb(II) remained constant within sample volume of 10−50 mL even for a very short contact time, for example, 10 min. Such features of GO-NH_2 nanosheets as wrinkled structure, flexibility, softness, and excellent dispersibility in water allow achieving very good contact with analyzed solution. In consequence, adsorption of Pb(II) ions and equilibrium state are achieved very fast. However, a decrease of adsorption percentage is observed for the sample volumes of 75 and 100 mL. Moreover, the adsorption decreases with time being shortened. To summarize, the analysis of real water samples can be performed using the sample volume from 10 to 50 mL (contact time 10 min) to obtain adequate enrichment factor and in consequence the detection limit fitted for the purpose.

After adsorption process, the GO-NH_2 with adsorbed Pb(II) ions was separated from the aqueous sample via filtration using membrane filter of 5 mm in diameter. The membrane filter with collected GO-NH_2 was placed in 3 mL-Eppendorf containing HNO_3 solution, and the closed Eppendorf was placed in ultrasonic bath for 2 min. For the subsequent analysis, two strategies were investigated:

- The suspension of GO-NH_2 was injected directly into the graphite tube and analyzed by ET-AAS.
- The redispersed GO-NH_2 was separated via filtration or centrifugation, and eluent was analyzed by ET-AAS.

In the second case, the effect of the volume and the concentration of HNO_3 on the recovery was investigated by varying eluent volume from 0.25 to 1 mL and the concentration from 0.5 to 2.0 mol L^{-1}. Figure 7b shows that Pb(II) ions can be quantitatively eluted using 0.5−1.0 mL of 1.0−2.0 mol L^{-1} HNO_3 with recovery of 95−98%. For lower concentration of HNO_3 (0.5 mol L^{-1}), the decrease of the recovery is observed (from 65 to 89%). To obtain satisfactory recovery and enrichment factor, 0.5 mL of 2.0 mol L^{-1} HNO_3 was chosen for subsequent analysis. Applied nitric acid can enhance deterioration of the graphite tube surface. However, during our experiment, we did not observe any shortening of lifetime of graphite tube. Of course, GO-NH_2 with adsorbed Pb(II) ions can also be redispersed in high-purity water if analysis is performed without elution of Pb(II) ions.

3.4. Analytical Method Validation. Analytical figures of merit of DMSPE procedure using GO-NH_2 as solid adsorbent are presented in Table 2. As can be seen, both strategies (direct ET-AAS analysis of GO-NH_2 suspension and analysis of solution after separation of GO-NH_2 solid phase) give very similar results. It is worth noting that some background signal caused by GO-NH_2 solid phase can be expected. However, the absorbance for blank sample of suspension (Abs = 0.114 ± 0.0048) is only a little higher than for eluted samples (Abs = 0.084 ± 0.0038). The limits of detection as well as limits of quantification (LOD and LOQ, respectively, calculated as the concentration corresponding to three and 10 times the standard deviation σ_B of 10 runs of the blank samples) allow for ultratrace determination of Pb(II) ions. The relative standard deviation (RSD) characterizing precision of the method obtained after analyzing a series of nine replicates is 4−5%, which can be considered as excellent for ultratrace

Table 2. Analytical Figures of Merit of SPE Procedure Using GO-NH_2 as Solid Adsorbent (20 μL of Aliquots or Suspensions Injected into the Graphite Tube)

	direct analysis of GO-NH_2 suspension	analysis after elution
recovery (%)	95.1 ± 5.0	96.3 ± 4.0
RSD (%) (n = 9, C = 250 ng L^{-1})	5.3	4.1
maximum enrichment factor	100	100
LOD, ng L^{-1} ($3\sigma_B$)	11.6	9.4
LOQ, ng L^{-1} ($10\sigma_B$)	38	31
linear range, ng mL^{-1}	2–30	2–30
equation (C in ng mL^{-1})	Abs = 0.0124 × C + 0.005	Abs = 0.0121 × C + 0.030
correlation coefficient	0.997	0.996

analysis. Taking into account both the LOD and precision, the method is suitable for the analysis of water samples. The accuracy of the analytical procedure was verified by the analysis of certified reference materials: LGC6016 (high salinity water—estuarine water from a heavily industrialized area) and groundwater (BCR-610). The results are presented in Table 3. The good agreement between certified and determined concentrations demonstrates the accuracy of the proposed method. The reliability of the analytical procedure was also examined by the analysis of river water and lake water with relatively high content of organic matter spiked with the known concentration of Pb(II). The results included in Table 4 show that the recoveries of Pb(II) are reasonable for ultratrace analysis. It is noteworthy that GO-NH_2 can be applied in the ultratrace analysis of high salinity water as well as in the presence of organic matter.

3.5. Comparison of GO-NH_2 and Other SPE Methods.

Carbon-based nanomaterials have received much attention for their potential applications in analytical chemistry. A comparison between the reported method and some recently published methods for Pb(II) ions determination using CNTs, fullerene, graphene, and GO is shown in Table 5. In most SPE methodologies, the liquid sample is passed through a column containing an adsorbent that retains the analytes.[58−67] However, very small particles of nanomaterial can cause high pressure in the SPE column, and nanoparticles can escape from the SPE cartridge, especially under high pressure. For these reasons, the application of highly hydrophilic GO nanosheets is seriously hampered or even impossible. These difficulties can be overcome by covalently binding GO nanosheets to support[68,69] or by the application of hollow fiber solid-phase microextraction.[70] In this paper, a methodology based on DMSPE was developed to solve these problems. The proposed procedure is very fast and requires a very small amount of nanomaterial in comparison to classical SPE (1 mg in DMSPE and 30−300 mg in SPE). As can be seen in Table 5, the proposed method has excellent LOD (even lower than ICP-MS) and very good precision. The impressive LOD results from the high preconcentration factor and application of ET-AAS as a measurement technique. Adsorption capacity is better compared to most other adsorbents. In contrast to raw CNTs,[58−61] fullerene,[66] and graphene,[67] the application of a chelating agent is not needed because of the presence of the nitrogen-containing groups on the surface of GO-NH_2.

Table 4. Determination of Pb(II) in Spiked Water Samples; n = 3; Uncertainties Correspond to One Standard Deviation

sample	added, (ng L^{-1})	found, (ng L^{-1})	recovery (%)
lake water	0	126 ± 12	
	100	234 ± 16	108
	200	320 ± 9	97
river water	0	208 ± 8	
	100	299 ± 12	91
	200	400 ± 14	96

4. CONCLUSIONS

GO was successfully modified through the amino-silanization with APTES. The experiments show that GO-NH_2 is characterized by high selectivity toward Pb(II) ions at pH 6. Adsorption isotherms suggest that sorption of Pb(II) ions on GO-NH_2 is monolayer coverage, and adsorption is controlled by chemical process involving the surface complexation of Pb(II) ions with the nitrogen-containing groups. The maximum adsorption capacity of 96 mg g^{-1} is lower than that for pure GO. However, the advantage of GO-NH_2 over GO is its high selectivity toward Pb(II). The adsorptive properties of GO-NH_2 indicate its potential for application as an adsorbent in analytical chemistry. In this work, the GO-NH_2 was used for selective and sensitive determination of Pb(II) ions by ET-AAS using DMSPE. Such features of GO-NH_2 nanosheets as wrinkled structure, softness, flexibility, and excellent dispersibility in water allow obtaining very good contact with analyzed solution, and adsorption of Pb(II) ions is achieved within 10 min. The experiment also shows that suspension GO-NH_2 with adsorbed Pb(II) ions can be directly injected into the graphite tube in ET-AAS system. In this way, the elution step can be avoided to eliminate additional chemical reagents. The developed methodology is characterized by extremely low LOD (9.4 ng L^{-1}) and a high degree of tolerance for sample matrix.

Table 3. ET-AAS Analysis of Certified Reference Materials (CRM), n = 3; Uncertainties Correspond to One Standard Deviation

			determined concentration, (ng g^{-1})		relative difference (%)	
CRM	matrix	certified concentration, ng g^{-1}	direct analysis of GO-NH_2 suspension	analysis after elution	direct analysis of GO-NH_2 suspension	analysis after elution
LGC6016[a]	4.7 mg g^{-1} Na, 0.57 mg g^{-1} Mg, 0.22 mg g^{-1} Ca, 0.18 mg g^{-1} K	196 ± 3	203 ± 8	199 ± 6	3.6	1.5
BCR-610[b]	major and minor elements are not given in certificate	7.78 ± 0.13	8.2 ± 0.58	7.5 ± 0.39	4.8	3.7

[a]estuarine water. [b]groundwater.

Table 5. Summary of Some Previous SPE Studies Using Carbon-Based Nanosorbents for Pb(II) Determination

adsorbent	chelating agent	EF[a]	LOD, ng mL^{-1}	RSD (%)	capacity, mg g^{-1}	technique	ref
150 mg of CNTs	dithizone	30	3.3	1.1	2.06	F-AAS[b]	58
200 mg of CNTs	*o*-cresolphthalein	40	3.5			F-AAS	59
300 mg of CNTs	APDC[c]	80	0.60	<5	10.3	F-AAS	60
200 mg of CNTs	violuric Acid	40	0.43	<10		F-AAS	61
50 mg of CNT-EDA[d]		200	0.3	1.9	54.5	ICP-OES[e]	62
30 mg of CNT-TAA[f]		60	0.3	3.5	38	ICP-OES	63
40 mg of CNT-ABTZ[g]		100	0.3	1.6	60	ICP-OES	64
30 mg of CNT-PIDA[h]		100	0.2	1.5	17.0	ICP-OES	65
40 mg of fullerene	APDC	200	2.4	<4.5		TS-F-AAS[i]	66
30 mg of graphene	dithizone	125	0.61	3.5	16.6	F-AAS	67
200 mg of GO@SiO_2		200	0.27	1.0	13.6	F-AAS	68
200 mg of GO@PS[j]		400	2.5	<5	228	F-AAS	69
GO-silica hollow fiber		10	0.028	4.6		ICP-MS[k]	70
1 mg of GO-NH_2		100	0.009	4−5	96	ET-AAS	this work

[a]Enrichment factor. [b]Flame atomic absorption spectrometry. [c]Ammonium pyrrolidine dithiocarbamate. [d]EDA: ethylenediamine. [e]Inductively coupled plasma atomic emission spectroscopy. [f]TAA: tris(2-aminoethyl)amine. [g]ABTZ: 2-aminobenzothiazole. [h]PIDA: phenyl-iminodiacetic acid. [i]Thermospray flame furnace atomic absorption spectrometry. [j]PS: polystyrene. [k]Inductively coupled plasma mass spectrometry.

AUTHOR INFORMATION

Corresponding Author

*Phone: +48 32 3591556. Fax: +48 32 2599978. E-mail: rafal.sitko@us.edu.pl.

Notes

The authors declare no competing financial interest.

ACKNOWLEDGMENTS

The project was supported by the National Science Center (Poland) by the Grant No. DEC-2012/07/B/ST4/00568.

REFERENCES

(1) Novoselov, K. S.; Geim, A. K.; Morozov, S. V.; Jiang, D.; Zhang, Y.; Dubonos, S. V.; Grigorieva, I. V.; Firsov, A. A. Electric Field in Atomically Thin Carbon Films. *Science* **2004**, *306*, 666−669.

(2) Geim, A. K.; Novoselov, K. S. The Rise of Graphene. *Nat. Mater.* **2007**, *6*, 183−191.

(3) Avouris, P.; Dimitrakopoulos, C. Graphene: Synthesis and Applications. *Mater. Today* **2012**, *15*, 86−97.

(4) Huang, Y.; Liang, J.; Chen, Y. An Overview of the Applications of Graphene-Based Materials in Supercapacitors. *Small* **2012**, *8*, 1805−1834.

(5) Jiang, H. Chemical Preparation of Graphene-Based Nanomaterials and Their Applications in Chemical and Biological Sensors. *Small* **2011**, *7*, 2413−2427.

(6) Brownson, D. A. C.; Banks, C. E. Graphene Electrochemistry: an Overview of Potential Applications. *Analyst* **2010**, *135*, 2768−2778.

(7) Machado, B. F.; Serp, P. Graphene-Based Materials for Catalysis. *Catal. Sci. Technol.* **2012**, *2*, 54−75.

(8) Luo, B.; Liu, S.; Zhi, L. Chemical Approaches Toward Graphene-Based Nanomaterials and their Applications in Energy-Related Areas. *Small* **2012**, *8*, 630−646.

(9) Chowdhury, S.; Balasubramanian, R. Recent Advances in the Use of Graphene-Family Nanoadsorbents for Removal of Toxic Pollutants from Wastewater. *Adv. Colloid Interface Sci.* **2014**, *204*, 35−56.

(10) Pei, Z.; Li, L.; Sun, L.; Zhang, S.; Shan, X.-Q.; Yang, S.; Wen, B. Adsorption Characteristics of 1,2,4-Trichlorobenzene, 2,4,6-Trichlorophenol, 2-Naphthol and Naphthalene on Graphene and Graphene Oxide. *Carbon* **2013**, *51*, 156−163.

(11) Yang, X.; Li, J.; Wen, T.; Ren, X.; Huang, Y.; Wang, X. Adsorption of Naphthalene and its Derivatives on Magnetic Graphene Composites and the Mechanism Investigation. *Colloids Surf., A* **2013**, *422*, 118−125.

(12) Ji, L.; Chen, W.; Xu, Z.; Zheng, S.; Zhu, D. Graphene Nanosheets and Graphite Oxide as Promising Adsorbents for Removal of Organic Contaminants from Aqueous Solution. *J. Environ. Qual.* **2013**, *42*, 191−198.

(13) Liu, Q.; Shi, J.; Jiang, G. Application of Graphene in Analytical Sample Preparation. *Trends Anal. Chem.* **2012**, *37*, 1−11.

(14) Sitko, R.; Zawisza, B.; Malicka, E. Graphene as a New Sorbent in Analytical Chemistry. *Trends Anal. Chem.* **2013**, *51*, 33−43.

(15) Pérez-López, B.; Merkoçi, A. Carbon Nanotubes and Graphene in Analytical Sciences. *Microchim. Acta.* **2012**, *179*, 1−16.

(16) Wang, X.; Liu, B.; Lu, Q.; Qu, Q. Graphene-Based Materials: Fabrication and Application for Adsorption in Analytical Chemistry. *J. Chromatogr., A* **2014**, *1362*, 1−15.

(17) Zhao, G.; Li, J.; Ren, X.; Chen, C.; Wang, X. Few-Layered Graphene Oxide Nanosheets as Superior Sorbents for Heavy Metal Ion Pollution Management. *Environ. Sci. Technol.* **2011**, *45*, 10454−10462.

(18) Wu, W.; Yang, Y.; Zhou, H.; Ye, T.; Huang, Z.; Liu, R.; Kuang, Y. Highly Efficient Removal of Cu(II) from Aqueous Solution by Using Graphene Oxide. *Water, Air, Soil Pollut.* **2013**, *224*, 1372−1379.

(19) Sitko, R.; Turek, E.; Zawisza, B.; Malicka, E.; Talik, E.; Heimann, J.; Gagor, A.; Feist, B.; Wrzalik, R. Adsorption of Divalent Metal Ions From Aqueous Solutions Using Graphene Oxide. *Dalton Trans.* **2013**, *42*, 5682−5689.

(20) Sun, Y.; Wang, Q.; Chen, C.; Tan, X.; Wang, X. Interaction Between Eu(III) and Graphene Oxide Nanosheets Investigated by Batch and Extended X-Ray Absorption Fine Structure Spectroscopy and by Modeling Techniques. *Environ. Sci. Technol.* **2012**, *46*, 6020−6027.

(21) Ding, C.; Cheng, W.; Sun, Y.; Wang, X. Determination of Chemical Affinity of Graphene Oxide Nanosheets with Radionuclides Investigated by Macroscopic, Spectroscopic and Modeling Techniques. *Dalton Trans.* **2014**, *43*, 3888−3896.

(22) Zhao, G.; Wen, T.; Yang, X.; Yang, S.; Liao, J.; Hu, J.; Shao, D.; Wang, X. Preconcentration of U(vi) Ions on Few-Layered Graphene Oxide Nanosheets from Aqueous Solutions. *Dalton Trans.* **2012**, *41*, 6182−6188.

(23) Li, Z.; Chen, F.; Yuan, L.; Liu, Y.; Zhao, Z.; Chai, Z.; Shi, W. Uranium(VI) Adsorption on Graphene Oxide Nanosheets from Aqueous Solutions. *Chem. Eng. J.* **2012**, *210*, 539−546.

(24) Zhao, G.; Ren, X.; Gao, X.; Tan, X.; Li, J.; Chen, C.; Huang, Y.; Wang, X. Removal of Pb(ii) Ions From Aqueous Solutions on Few-Layered Graphene Oxide Nanosheets. *Dalton Trans.* **2011**, *40*, 10945−10952.

(25) Madadrang, C. J.; Kim, H. Y.; Gao, G.; Wang, N.; Zhu, J.; Feng, H.; Gorring, M.; Kasner, M. L.; Hou, S. Adsorption Behavior of

EDTA-Graphene Oxide for Pb(II) Removal. *ACS Appl. Mater. Interfaces* **2012**, *4*, 1186−1193.
(26) Zhang, F.; Wang, B.; He, S.; Man, R. Preparation of Graphene-Oxide/Polyamidoamine Dendrimers and Their Adsorption Properties toward Some Heavy Metal Ions. *J. Chem. Eng. Data* **2014**, *59*, 1719−1726.
(27) Zhang, Y.; Chi, H.; Zhang, W.; Sun, Y.; Liang, Q.; Gu, Y.; Jing, R. Highly Efficient Adsorption of Copper Ions by a PVP-Reduced Graphene Oxide Based on a New Adsorptions Mechanism. *Nano-Micro Lett.* **2014**, *6*, 80−87.
(28) Musico, Y. L. F.; Santos, C. M.; Dalida, M. L. P.; Rodrigues, D. F. Improved Removal of Lead(ii) From Water Using a Polymer-Based Graphene Oxide Nanocomposite. *J. Mater. Chem. A* **2013**, *1*, 3789−3796.
(29) Mejias Carpio, I. E.; Mangadlao, J. D.; Nguyen, H. N.; Advincula, R. C.; Rodrigues, D. F. Graphene Oxide Functionalized with Ethylenediamine Triacetic Acid for Heavy Metal Adsorption and Anti-Microbial Applications. *Carbon* **2014**, *77*, 289−301.
(30) Qin, H.; Gong, T.; Cho, Y.; Lee, C.; Kim, T. A Conductive Copolymer of Graphene Oxide/Poly(1-(3-aminopropyl)pyrrole) and the Adsorption of Metal Ions. *Polym. Chem.* **2014**, *5*, 4466−4473.
(31) Liu, G.; Gui, S.; Zhou, H.; Zeng, F.; Zhou, Y.; Ye, H. A Strong Adsorbent for Cu^{2+}: Graphene Oxide Modified with Triethanolamine. *Dalton Trans.* **2014**, *43*, 6977−6980.
(32) Gui, C.-H.; Wang, Q.-Q.; Hao, S.-M.; Qu, J.; Huang, P.-P.; Cao, C.-Y.; Song, W.-G.; Yu, Z.-Z. Sandwichlike Magnesium Silicate/Reduced Graphene Oxide Nanocomposite for Enhanced Pb^{2+} and Methylene Blue Adsorption. *ACS Appl. Mater. Interfaces* **2014**, *6*, 14653−14659.
(33) Liu, L.; Li, C.; Bao, C.; Jia, Q.; Xiao, P.; Liu, X.; Zhang, Q. Preparation and Characterization of Chitosan/Graphene Oxide Composites for the Adsorption of Au(III) and Pd(II). *Talanta* **2012**, *93*, 350−357.
(34) Fan, L.; Luo, C.; Sun, M.; Qiu, H. Synthesis of Graphene Oxide Decorated with Magnetic Cyclodextrin for Fast Chromium Removal. *J. Mater. Chem.* **2012**, *22*, 24577−24583.
(35) Chandra, V.; Park, J.; Chun, Y.; Lee, J. W.; Hwang, I.-C.; Kim, K. S. Water-**D**ispersible Magnetite-Reduced Graphene Oxide Composites for Arsenic Removal. *ACS Nano* **2010**, *4*, 3979−3986.
(36) Li, J.; Zhang, S.; Chen, C.; Zhao, G.; Yang, X.; Li, J.; Wang, X. Removal of Cu(II) and Fulvic Acid by Graphene Oxide Nanosheets Decorated with Fe_3O_4 Nanoparticles. *ACS Appl. Mater. Interfaces* **2012**, *4*, 4991−5000.
(37) Bao, J.; Fu, Y.; Bao, Z. Thiol-Functionalized Magnetite/Graphene Oxide Hybrid as a Reusable Adsorbent for Hg^{2+} Removal. *Nanoscale Res. Lett.* **2013**, *8*, 486−491.
(38) Marcano, D. C.; Kosynkin, D. V.; Berlin, J. M.; Sinitskii, A.; Sun, Z.; Slesarev, A.; Alemany, L. B.; Lu, W.; Tour, J. M. Improved Synthesis of Graphene Oxide. *ACS Nano* **2010**, *4*, 4806−4814.
(39) Li, Z.; Wang, R.; Young, R. J.; Deng, L.; Yang, F.; Hao, L.; Jiao, W.; Liu, W. Control of the Functionality of Graphene Oxide for its Application in Epoxy Nanocomposites. *Polymer* **2013**, *54*, 6437−6446.
(40) Hong, S. M.; Kim, S. H.; Lee, K. B. Adsorption of Carbon Dioxide on 3-Aminopropyl-triethoxysilane Modified Graphite Oxide. *Energy Fuels* **2013**, *27*, 3358−3363.
(41) Ju, H.-M.; Choi, S.-H.; Huh, S. H. X-Ray Diffraction Patterns of Thermally-Reduced Graphenes. *J. Korean Phys. Soc.* **2010**, *57*, 1649−1652.
(42) Ju, H. M.; Huh, S. H.; Choi, S. H.; Lee, H. L. Structures of Thermally and Chemically Reduced Graphene. *Mater. Lett.* **2010**, *64*, 357−360.
(43) Reich, S.; Thomsen, C. Raman Spectroscopy of Graphite. *Philos. Trans. R. Soc., A* **2004**, *362*, 2271−2288.
(44) Ferrari, A. C. Raman Spectroscopy of Graphene and Graphite: Disorder, Electron−Phonon Coupling, Doping and Nonadiabatic Effects. *Solid State Commun.* **2007**, *143*, 47−57.
(45) Ferrari, A. C.; Robertson, J. Interpretation of Raman Spectra of Disordered and Amorphous Carbon. *Phys. Rev. B* **2000**, *61*, 14095−14107.
(46) Cançado, L. G.; Jorio, A.; Martins Ferreira, E. H.; Stavale, F.; Achete, C. A.; Capaz, R. B.; Moutinho, M. V. O.; Lombardo, A.; Kulmala, T. S.; Ferrari, A. C. Quantifying Defects in Graphene via Raman Spectroscopy at Different Excitation Energies. *Nano Lett.* **2011**, *11*, 3190−3196.
(47) Kudin, K. N.; Ozbas, B.; Schniepp, H. C.; Prud'homme, R. K.; Aksay, I. A.; Car, R. Spectra of Graphite Oxide and Functionalized Graphene Sheets. *Nano Lett.* **2008**, *8*, 36−41.
(48) Iqbal, M. Z.; Katsiotis, M. S.; Alhassan, S. M.; Liberatore, M. W.; Abdala, A. A. Effect of Solvent on the Uncatalyzed Synthesis of Aminosilane-Functionalized Graphene. *RSC Adv.* **2014**, *4*, 6830−6839.
(49) Zarrin, H.; Higgins, D.; Jun, Y.; Chen, Z.; Fowler, M. Functionalized Graphene Oxide Nanocomposite Membrane for Low Humidity and High Temperature Proton Exchange Membrane Fuel Cells. *J. Phys. Chem. C* **2011**, *115*, 20774−20781.
(50) Liu, Z.; Duan, X.; Qian, G.; Zhou, X.; Yuan, W. Eco-Friendly One-Pot Synthesis of Highly Dispersible Functionalized Graphene Nanosheets with Free Amino Groups. *Nanotechnology* **2013**, *24*, 045609.
(51) Wu, L.; Zhang, B.; Lu, H.; Liu, C.-Y. Nanoscale Ionic Materials Based on Hydroxyl-Functionalized Graphene. *J. Mater. Chem. A* **2014**, *2*, 1409−1417.
(52) Jiang, Z.; Zhao, X.; Manthiram, A. Sulfonated Poly(ether ether ketone) Membranes with Sulfonated Graphene Oxide Fillers for Direct Methanol Fuel Cells. *Int. J. Hydrogen Energy* **2013**, *38*, 5875−5884.
(53) Zhu, J.; Yang, J.; Deng, B. Enhanced Mercury Ion Adsorption by Amine-Modified Activated Carbon. *J. Hazard. Mater.* **2009**, *166*, 866−872.
(54) Ho, Y. S.; McKay, G. Pseudo-Second Order Model for Sorption Processes. *Process Biochem.* **1999**, *34*, 451−465.
(55) Langmuir, I. The Constitution and Fundamental Properties of Solids and Liquids. *J. Am. Chem. Soc.* **1916**, *38*, 2221−2295.
(56) Langmuir, I. Adsorption of Gases on Plain Surfaces of Glass Mica Platinum. *J. Am. Chem. Soc.* **1918**, *40*, 1361−1403.
(57) Freundlich, H. M. F. Uber die Adsorption in Lasugen. *Z. Phys. Chem.* **1906**, *57*, 385−470.
(58) Tavallali, H.; Asvad, H. Flame Atomic Absorption Spectrometric Determination of Trace Amounts of Pb (II) after Soild Phase Extraction Using Multiwalled Carbon Nanotube. *Int. J. ChemTech Res.* **2011**, *3*, 1635−1640.
(59) Duran, A.; Tuzen, M.; Soylak, M. Preconcentration of Some Trace Elements via Using Multiwalled Carbon Nanotubes as Solid Phase Extraction Adsorbent. *J. Hazard. Mater.* **2009**, *169*, 466−471.
(60) Tuzen, M.; Saygi, K. O.; Soylak, M. Solid Phase Extraction of Heavy Metal Ions in Environmental Samples on Multiwalled Carbon Nanotubes. *J. Hazard. Mater.* **2008**, *152*, 632−639.
(61) Soylak, M.; Murat, I. Determination of Copper, Cobalt, Lead, and Iron in Table Salt by FAAS After Separation Using Violuric Acid and Multiwalled Carbon Nanotubes. *Food Anal. Methods* **2012**, *5*, 1003−1009.
(62) Zang, Z.; Hu, Z.; Li, Z.; He, Q.; Chang, X. Synthesis, Characterization and Application of Ethylenediamine-Modified Multiwalled Carbon Nanotubes for Selective Solid-Phase Extraction and Preconcentration of Metal Ions. *J. Hazard. Mater.* **2009**, *172*, 958−963.
(63) Cui, Y.; Liu, S.; Hu, Z.-J.; Liu, X.-H.; Gao, H.-W. Solid-Phase Extraction of Lead(II) Ions Using Multiwalled Carbon Nanotubes Grafted with Tris(2-aminoethyl)amine. *Microchim. Acta* **2011**, *174*, 107−113.
(64) Li, R.; Chang, X.; Li, Z.; Zang, Z.; Hu, Z.; Li, D.; Tu, Z. Multiwalled Carbon Nanotubes Modified with 2-Aminobenzothiazole Modified for Uniquely Selective Solid-Phase Extraction and Determination of Pb(II) Ion in Water Samples. *Microchim. Acta* **2011**, *172*, 269−276.
(65) Cui, Y.; Hu, Z.-J.; Yang, J.-X.; Gao, H.-W. Novel Phenyl-Iminodiacetic Acid Grafted Multiwalled Carbon Nanotubes for Solid Phase Extraction of Iron, Copper and Lead Ions from Aqueous Medium. *Microchim. Acta* **2012**, *176*, 359−366.

(66) Pereira, M. G.; Pereira-Filho, E. R.; Berndt, H.; Arruda, M. A. Z. Determination of Cadmium and Lead at Low Levels by Using Preconcentration at Fullerene Coupled to Thermospray Flame Furnace Atomic Absorption Spectrometry. *Spectrochim. Acta, Part B* **2004**, *59*, 515−521.
(67) Wang, Y.; Gao, S.; Zang, X.; Li, J.; Ma, J. Graphene-Based Solid-Phase Extraction Combined with Flame Atomic Absorption Spectrometry for a Sensitive Determination of Trace Amounts of Lead in Environmental Water and Vegetable Samples. *Anal. Chim. Acta* **2012**, *716*, 112−118.
(68) Sitko, R.; Zawisza, B.; Talik, E.; Janik, P.; Osoba, G.; Feist, B.; Malicka, E. Spherical Silica Particles Decorated with Graphene Oxide Nanosheets as a New Sorbent in Inorganic Trace Analysis. *Anal. Chim. Acta* **2014**, *834*, 22−29.
(69) Islam, A.; Ahmad, H.; Zaidi, N.; Kumar, S. Graphene Oxide Sheets Immobilized Polystyrene for Column Preconcentration and Sensitive Determination of Lead by Flame Atomic Absorption Spectrometry. *ACS Appl. Mater. Interfaces* **2014**, *6*, 13257−13265.
(70) Su, S.; Chen, B.; He, M.; Hu, B. Graphene Oxide-Silica Composite Coating Hollow Fiber Solid Phase Microextraction Online Coupled with Inductively Coupled Plasma Mass Spectrometry for the Determination of Trace Heavy Metals in Environmental Water Samples. *Talanta* **2014**, *123*, 1−9.